Agricultural and Forest Meteorology 216 (2016) 82–92

Contents lists available at ScienceDirect

Agricultural and Forest Meteorology

journal homepage: www.elsevier.com/locate/agrformet

Assessment of foliage clumping effects on evapotranspiration estimates in forested ecosystems

Bin Chen[a,c,*], Jane Liu[b,c,**], Jing M. Chen[c], Holly Croft[c], Alemu Gonsamo[c], Liming He[c], Xiangzhong Luo[c]

[a] International Institute for Earth System Science, Nanjing University, Nanjing, China
[b] School of Atmospheric Sciences, Nanjing University, Nanjing, China
[c] Department of Geography and Program in Planning, University of Toronto, Toronto, Canada

ARTICLE INFO

Article history:
Received 21 April 2015
Received in revised form
21 September 2015
Accepted 24 September 2015
Available online 11 November 2015

Keywords:
Canopy structure
Canopy radiation regime
Water vapor flux
Eddy covariance
Leaf energy balance
Stomata conductance

ABSTRACT

In forested ecosystems, the aggregation of leaves into different spatial structures at the canopy, branch and shoot scales leads to a non-random spatial distribution of foliar elements. However, effect of foliar aggregation or clumping on the estimation of terrestrial evapotranspiration (ET) is not yet well understood. To evaluate the effect of foliar clumping, the process-based Boreal Ecosystem Productivity Simulator (BEPS) is used to simulate ET at eight flux tower sites in North American forests. BEPS separates a canopy into sunlit and shaded leaf groups in the calculation of canopy-level ET and clumping affects this separation. Three cases are simulated with BEPS, and the modeled ET values are compared with flux tower measurements: Case I serves as a baseline, in which LAI and clumping index at the sites are considered. In this case, BEPS can explain 43–75% the variance of measured ET at these sites. For Case II, the LAI is considered but clumping is ignored; resulting in an overestimation of annual ET at all sites by ~5% at the most clumped sites. In Case III, when effective LAI is used (i.e. clumping is not considered), the site-averaged mean annual ET is underestimated by 11.5%, with the largest underestimation found at the site with most clumping (CA-DF49; 19.1%). In both Case II and Case III, the more clumped a canopy is, the larger bias is found in the ET estimation ($p < 0.001$). The estimated biases are robust to the errors in key driving variables and model parameters. When LAI is derived from optical measurements on the ground and from satellite platforms without considering the effect of clumping, it can cause substantial underestimation of ET.

These results demonstrate the need for considering foliage clumping in process-based ET modeling, with potential biases having large implications for carbon cycle modeling, water budget calculations and understanding and predicting ecosystem responses to future climatic scenarios.

1. Introduction

Terrestrial evapotranspiration (ET) is the process by which water is transferred from the vegetated land surface to the atmosphere, through a phase change of water from liquid (or ice) to gas (water vapor). ET is instrumental in controlling soil moisture and vegetation productivity, and plays a pivotal role in the carbon cycle and water budgets within terrestrial ecosystems, by absorbing energy and cooling the land surface (Yuan et al., 2010; Wang and Dickinson, 2012). Terrestrial ET estimates can be derived using process-based ecosystem models, which simulate a series of biophysical and plant physiological processes, including radiation regime, precipitation interception and surface resistance (Ju et al., 2006; Liu et al., 2003, 1997; Running and Coughlan, 1988; Ryu et al., 2011; Sellers et al., 1997; Chen et al., 2007; Potter et al., 2001). Based on the combination of heat and mass transfer and energy balance equations, the Penman-Monteith (PM) equation (Monteith, 1965) is widely adopted to estimate ET in those ecosystem models. Whilst the PM equation is theoretically sound, its application, particularly for large areas, still faces several challenges. One of them relates to the scaling scheme for canopy ET estimation. A traditional way is to treat the entire canopy as a big leaf (Raupach

* Corresponding author at: International Institute for Earth System Science, Nanjing University, Nanjing, China.
** Corresponding author at: School of Atmospheric Sciences, Nanjing University, Nanjing, China.
E-mail addresses: classgg.temp@gmail.com (B. Chen), janejj.liu@utoronto.ca (J. Liu).

http://dx.doi.org/10.1016/j.agrformet.2015.09.017
0168-1923/

and Finnigan, 1988). A bulk stomatal resistance and a bulk aerodynamic resistance must be specified a priori in the big-leaf approach. Although the big-leaf approach is simple and effective and has been widely used for ET estimation (Band et al., 1991; Kelliher et al., 1995; Lai et al., 2000; Running and Coughlan, 1988), it is often difficult to determine the values of the bulk aerodynamic and canopy resistances that are reliable for variable environmental and canopy structural conditions (Paw and Meyers, 1989).

A two-leaf scheme was proposed as an alternative (Chen et al., 1999, 2005; Liu et al., 2003), in which ET is estimated for the sunlit and shaded representative leaves separately, then scaled up by their respective leaf areas. Thus, ET is calculated at leaf level and stomatal resistance is used as the surface resistance in the PM equation. This scheme can make the water and carbon cycles tightly coupled and achieve high efficiency for large area applications (Liu et al., 2003; Ryu et al., 2011; Liu et al., 2013).

Another challenge in the application of the PM equation is to accurately describe the vegetation canopy structure. Leaf area index (LAI) representing the vegetation amount is defined as one half of the total leaf area per unit ground surface area projected to horizontal datum (Chen and Black, 1992). LAI is recognized as the most important canopy structural parameter in ET estimation because it determines the surface area where fluxes of water vapor and CO_2 occur between the plants and the atmosphere. LAI also greatly modulates radiation transfer in plant canopy and precipitation interception by the canopy, and LAI is related to the total wet and dry leaf area for estimating canopy evaporation and transpiration, respectively (Mu et al., 2011). However, in order to correctly calculate LAI values, the aggregation of leaves into different spatial structures i.e. twigs, branches, tree crowns and groups of trees, must be accounted for. The foliage clumping index (Ω), quantifies the degree of deviation of foliage spatial distribution from the random case (Chen and Black, 1991; Chen et al., 2006). The effects of foliage clumping have been overlooked in ET estimations in most ecosystem models (Lai et al., 2000; Sellers et al., 1997) but have attracted some attention recently (Ryu et al., 2011).

Foliage clumping is needed for accurate ET estimation for three reasons: firstly, the clumping index is needed to derive LAI from the effective LAI (LAI_e) which can be measured with optical instruments at the ground or from satellite platforms (Chen and Black, 1992; Chen, 1996a):

$$LAI = \frac{(1-\alpha)LAI_e}{\Omega} \quad (1)$$

where α is the woody-to-total area ratio. The range of foliage clumping index (Ω) is between 0 and 1. The more clumped a forest is, the smaller the clumping index. Ω is around 0.5 for conifer forests, which usually have high clumped canopies (Black et al., 1991). LAI would therefore be considerably underestimated for a highly clumped canopy (i.e. conifer forests) if foliage clumping is ignored.

Secondly, Ω is used in the separation of sunlit and shaded portion of the canopy as follows (Chen et al., 1999):

$$LAI_{sun} = 2\cos\theta(1 - e^{-0.5\Omega LAI/\cos\theta}) \quad (2a)$$

$$LAI_{shade} = LAI - LAI_{sun} \quad (2b)$$

where the subscripts 'sun' and 'shade' denote the sunlit and shaded portion of LAI and θ is the solar zenith angle. For a highly clumped canopy (i.e. conifer forests), LAI_{sun} would be overestimated while LAI_{shade} would be underestimated for a given LAI when foliage clumping is ignored. LAI_{sun} and LAI_{shade} are used in the calculation of evaporation and transpiration rates of sunlit and shaded portions of the canopy. Thus, we would expect that the inaccurate calculation of LAI_{sun} and LAI_{shade} would introduce errors into the estimation of canopy ET.

Thirdly, Ω is needed to accurately simulate radiation transfer inside plant canopies (see Appendix A). For example, a simple radiation transfer model can be written as:

$$P(\theta) = e^{-G(\theta)\Omega LAI/\cos\theta} \quad (3)$$

where $P(\theta)$ represents the probability of radiation transmission through the canopy at the solar zenith angle θ. $G(\theta)$ is the projection coefficient, defined as the area projected on a plane perpendicular to the direction of radiation per unit leaf area, and taken as 0.5 for a spherical leaf angle distribution. In a clumped canopy, the grouping of leaves in the sub-canopy scales causes more overlapping of leaves in the vertical or any direction than the random case; therefore, increasing the probability of radiation transmission through the canopy. Thus, Ω influences the fraction of radiation intercepted by the canopy or allocated to lower layers, and therefore the amount of the radiation energy available for canopy evaporation or transpiration. Ω is especially important for diffuse radiation interception by the canopy (Eq. (A7)) and thus is important for ET estimation in cloudy days when the diffuse radiation is the significant portion of the incoming global solar radiation.

Given the influence of foliage aggregation on canopy spatial organization and consequent energy and water fluxes between the canopy and atmosphere, it is necessary to investigate the foliage clumping on the estimation of ET over forests, which contribute a large portion of the global ET. There are two types of biases associated with ignoring clumping in ET estimation. The first is to ignore clumping while LAI is considered. The other is to mistake the effective LAI as the true derived LAI. This type of bias can occur with optical measurements of LAI on the ground and from satellite platforms if the clumping index is assumed to be one. Therefore, the specific objectives of this study are (1) to quantify the magnitudes of these two types of biases in the estimation of site-level ET in North America using a process-based ecosystem model, and (2) to test the robustness of such bias estimates with errors in input and model parameters. This research will provide an important step for evaluating the effects of foliage clumping on ET estimation in ecosystem process models and lead to improved accuracies of ET estimation of forest ecosystems.

2. Materials and methods

2.1. Studied sites and vegetation parameters

In this study, we selected 8 North American eddy covariance (EC) flux tower sites, which are part of the Ameriflux and Canadian Carbon Program networks (Table 1). These 8 sites have a large range of clumping index (0.49–0.87) and have multiple biome types. Most of the sites have the ground-based measurements of clumping index and LAI which would be more accurate compared to those derived from remote sensing products. The sites span from northern boreal latitudes (54° N) to mid-latitudes (42° N). These sites include one boreal deciduous broadleaf forest: the Old Aspen site (CA-SOA, Prince Albert National Park, SK, Canada) and one temperate deciduous broadleaf forest: Harvard Forest (US-Ha1, MA, USA), three boreal evergreen conifer forests: BERMS – Old Black Spruce (CA-SOBS, SK, Canada), BERMS – Old Jack Pine (CA-SOJP, SK, Canada) and Quebec – Mature Black Spruce (CA-EOBS, QC, Canada) and three temperate evergreen conifer forests: Turkey Point – Mature (CA-TP39, ON, Canada), Metolius – Intermediate-aged Ponderosa Pine (US-Me2, OR, USA), and 1949 Douglas-fir stand (CA-DF49, BC, Canada). The mean annual temperature of these eight sites ranges from 0.0 °C at CA-EOBS site to 8.5 °C at US-Ha1 site. The mean annual precipitation ranges from 467 mm at the three boreal forest sites to 1461 mm at CA-DF49 site.

Table 1
Description of studied Canadian Carbon Program (CCP) and Ameriflux Flux Tower Sites[a].

Site ID	Location	Veg. type[a]	Clumping index	LAI_{max} [b]	LAI_u [b]	V_m [b] ($\mu mol\ m^{-2}\ s^{-1}$)	m[b]	Climate zone	Precip[b] (mm)	T_{air} [b] (°C)	Reference
CA-SOA	53.63° N, 106.20° W	DBF	0.870	2.1	1.88	95.9	8.0	Boreal	467	0.4	Barr et al. (2004)
US-Ha1	42.54° N, 72.17° W	DBF	0.70[c]	3.0	1.68	51.5	8.0	Temperate	1050	8.5	Davidson et al. (2006)
CA-SOBS	53.99° N, 105.12° W	ENF	0.660	3.8	0.03	30.0	8.0	Boreal	467	0.4	Bergeron et al. (2007)
CA-SOJP	53.92° N, 104.69° W	ENF	0.600	2.6	0.00	45.0	7.5	Boreal	467	0.4	Baldocchi et al. (1997)
CA-EOBS	49.69° N, 74.34° W	ENF	0.586	3.7	0.03	32.3	9.0	Boreal	961	0.0	Bergeron et al. (2007)
CA-TP39	42.71° N, 80.36° W	ENF	0.513	8.0	0.00	31.0	8.0	Temperate	800	8.1	Arain and Restrepo-Coupe (2005)
US-Me2	44.32° N, 121.61° W	ENF	0.51[c]	7.1	0.2	62.5	8.0	Temperate	489	7.3	Thomas et al. (2009)
CA-DF49	49.87° N, 25.33° W	ENF	0.488	7.3[d]	1.3[e]	54.1	8.0	Temperate	1461	8.3	Chen et al. (2009)

[a] Vegetation type: DBF, deciduous broadleaf forest; ENF, evergreen needleleaf forest.
[b] Precip: Mean Annual Precipitation; Tair: Mean Annual Air Temperature; LAI_{max}: summer overstory LAI; LAI_u: summer understory LAI; V_m is the maximum carboxylation rate at 25 °C; m is the slope in the BWB stomatal conductance model.
[c] Data were extracted from a global MODIS derived clumping index map at 500 m spatial resolution (He et al., 2012).
[d] From Chen et al. (2006).
[e] From destructive LAI measurement.

The EC tower sites were selected to give a comprehensive range of forest canopy structure and to fulfill the following conditions in data quality and availability: (1) ground measurements of LAI and Ω are available; (2) soil data including temperature, moisture, and texture are available; (3) three or more years of continuous measurements of carbon and water fluxes and meteorological variables, including downward shortwave radiation, air temperature, precipitation, wind speed and relative humidity are available; (4) the simulation periods were selected when 90% of the half-hourly data in any year are available for any meteorological variable and the latent heat flux (LE).

The overstory LAI_e was measured using the optical LAI-2000 plant canopy analyser (Li-Cor, Lincoln, NE, USA). The overstory Ω was derived from ground-based measurements using the Tracing Radiation and Architecture of Canopies (TRAC) instrument (Chen and Cihlar, 1995). The overstory LAI values were calculated using Eq. (1) (Table 1, Fig. 1). The measured mid-summer LAI values were used to determine the seasonal time series of LAI according to air temperature (Ju et al., 2006). Ω was measured using ground based optical instruments at most of the sites except for US-Me2 site where the measurement is not available and Ω was extracted from a global MODIS derived Ω map at 500 m spatial resolution (He et al., 2012).

The understory LAI at CA-SOA site is the mean value of LAI_e taken from leafed-out canopy for all years (1997–2005). The understory LAI at US-Ha1 site is the mean value of understory LAI_e (total LAI_e – overstory LAI_e) for all measurement years (1998–2008). At sites where the measurements were not available, the understory LAI was estimated using the empirical equation in Liu et al. (2003):

$$LAI_u = 1.1749e^{-0.9909LAI_o} \quad (4)$$

where the subscripts 'o' and 'u' are for overstory and understory, respectively. The understory LAI at SOJP site is set as 0.1 (Baldocchi et al., 1997).

2.2. Ecosystem modeling

ET was simulated using the Boreal Ecosystem Productivity Simulator (BEPS) (Liu et al., 1999, 2003; Chen et al., 1999) at half-hourly time steps for each site. BEPS is a two-leaf enzyme kinetic terrestrial ecosystem model designed to simulate the carbon and water cycles using spatial data sets of meteorology, remotely-sensed land surface variables, soil properties, and photosynthesis and respiration parameters. Although the BEPS model was initially developed for boreal forest ecosystems, it has since been substantially advanced (Ju et al., 2006; Chen et al., 2007) and intensively tested over the Canadian landmass (Gonsamo et al., 2013) and temperate and tropical environments (Feng et al., 2007; Wang et al., 2004; Zhou et al., 2007). The PM equation (Monteith, 1965) is used in BEPS to estimate the ET rate at an instant time per unit surface area (in $kg\ m^{-2}\ s^{-1}$):

$$ET = \left[\frac{\Delta R_n + (\rho_a c_p(e_s - e_a)/r_a)}{\Delta + \gamma(1 + (r_s/r_a))}\right] / \lambda_v \quad (5)$$

where R_n is the net absorbed radiation in $W\ m^{-2}$, e_s is the saturation vapor pressure (kPa) at the evaporating surface, e_a is the actual vapor pressure (kPa) of the air above the evaporating surface, r_a is aerodynamic resistance ($s\ m^{-1}$). The following parameters are treated as constants: Δ is gradient of the saturated water vapor curve with temperature in $kPa\ °C^{-1}$ ($\approx 0.155\ kPa\ °C^{-1}$); γ is the psychometric constant ($\approx 0.067\ kPa\ °C^{-1}$); λ_v is latent heat of vaporization ($\approx 2.45\ MJ\ kg^{-1}$); ρ_a is air density ($\approx 1.2\ kg\ m^{-3}$ at sea level); c_p is specific heat of air at constant pressure ($1.013 \times 10^{-3}\ MJ\ kg^{-1}\ °C^{-1}$). r_s is surface resistance ($s\ m^{-1}$); a key variable in the ET estimation. The surface resistance to the evaporation from the ground surface is termed as soil surface resistance (r_{soil}) as follows (Sellers et al., 1992):

$$r_{soil} = e^{8.206 - 4.255 \times (\theta_1/\theta_s)} \quad (6)$$

where θ_1 is volumetric soil water content in the first layer ($m^3\ m^{-3}$), and θ_s is saturated soil water content (equal to porosity) of the first soil layer ($m^3\ m^{-3}$).

The transpiration from the leaf is coupled with CO_2 uptake by the leaf through stomatal conductance (reciprocal of stomatal resistance), which can be described using the Ball–Woodrow–Berry (BWB) model (Ball, 1988):

$$g_s = \frac{1}{r_s} = m\frac{Ah_s}{C_s}P + g_0 \quad (7)$$

where g_s is stomatal conductance in $\mu mol\ m^{-2}\ s^{-1}$, A is net photosynthesis rate in $\mu mol\ m^{-2}\ s^{-1}$, m is a slope constant, h_s is relative humidity at leaf surface, p is atmospheric pressure, C_s is CO_2 concentration at the leaf surface and g_0 is a small intercept term. The

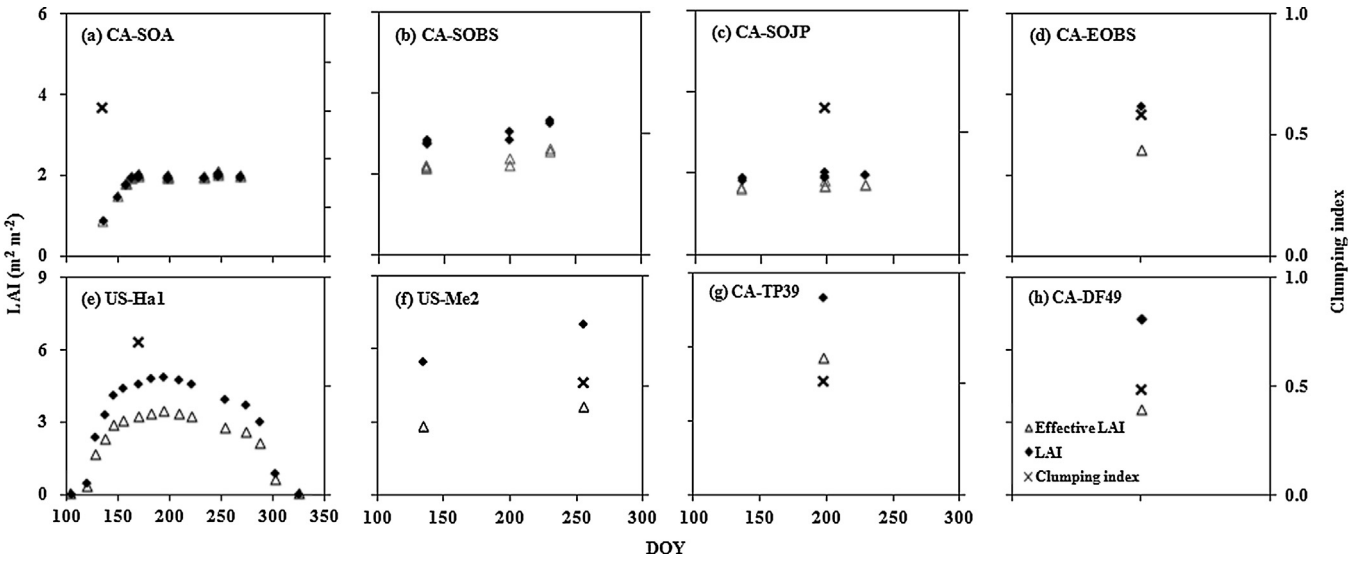

Fig. 1. LAI_e, LAI and clumping index across a growing season for each site. (a) CA-SOA site in 1997; (b) CA-SOBS site in 2001; (c) CA-SOJP site in 2001; (d) CA-EOBS site in 2003; (e) US-Ha1 site in 2010; (f) US-Me2 site in 2002; (g) CA-TP39 site in 2005; (h) CA-DF49 site in 2004.

slope constant m, and intercept g_0 vary between species. As g_s is needed in A calculation and A is needed in g_s calculation, an iteration procedure is usually followed for simultaneous estimations of A and g_s (Collatz et al., 1991). In this study, the value of g_s is obtained in this way for the sunlit and shaded representative leaves, respectively. An analytical solution of g_s (Baldocchi, 1994) was used in BEPS to improve the computation efficiency for model simulation at continental and global scales (Chen et al., 2012).

Canopy-level ET is the sum of ET for sunlit and shaded leaf groups as follows:

$$ET_{canopy} = ET_{sun}LAI_{sun} + ET_{shade}LAI_{shade} \quad (8)$$

where the subscripts 'sun' and 'shade' denote the sunlit and shaded components of canopy ET. This two-leaf formulation is based on the estimation of ET rates of a representative sunlit leaf (ET_{sun}) and a representative shaded leaf (ET_{shade}).

In BEPS, the total site-level ET is calculated as the sum of several components as follows:

$$ET = T_o + T_u + E_o + E_u + S_o + S_u + E_g + S_g \quad (9)$$

where T_o and T_u are the transpiration from overstory and understory canopies, respectively. E_o and E_u are the evaporation from overstory and understory canopy intercepted water, respectively. S_o and S_u are the sublimation from overstory and understory canopy intercepted snow, respectively. E_g is the evaporation from the ground surface and S_g is the sublimation from the snow on the ground.

2.3. Simulation cases

For the purpose of investigating the impact of foliage clumping on the ET estimation, we conducted model simulations for three cases (Table 2). In Case I, Ω is considered and LAI_e derived from optical instruments (i.e. the Tracing Radiation and Architecture of Canopy, TRAC or LAI-2000) is converted to LAI (Eq. (1)) using Ω measured at the ground (7 sites) or derived from the satellite data (1 site). Ω is also used in sunlit and shaded LAI separation. This case is considered to be unbiased and representative of reality.

Table 2
The model simulation cases.

Simulation cases	Clumping effects	LAI treatments
Case I	Considered	LAI is used.
Case II	Not considered	LAI is used.
Case III	Not considered	Effective LAI is used.

In Case II, the same LAI in case I is used, but the clumping is ignored assuming Ω equals to 1. This is the case that the LAI is available such as those obtained through destructive sampling or using allometric equations but a random leaf spatial distribution is assumed. Case II would result in overestimated LAI_{sun} (Eq. (2a)) and underestimated LAI_{shade} (Eq. (2b)) for a given LAI and the forest is highly clumped. In Case III, LAI_e derived from optical instruments is used and Ω is taken as 1. In this case, LAI_{sun} is unbiased (Eq. (2a)) whereas LAI_{shade} is underestimated (Eq. (2b)). In sum, the importance of foliage clumping in ET estimation is examined in two ways: using only LAI (Case II) or LAI_e (Case III) without consideration of clumping. Case III may be particularly relevant to site-level ET estimation using optical instrument data as the data derived from the optical instrument (i.e. LAI-2000) indicates the LAI_e while the LAI remains unknown.

3. Results and discussion

3.1. Variations in canopy structural variables between sites

The canopy structural variables (i.e. LAI, LAI_e, and Ω) are involved in the ET calculation in BEPS. Their values at the studied sites are shown in Fig. 1 and Table 1. The seasonal trajectory of leaf emergence, leaf growth, the peak of overstory LAI and leaf senescence were well captured at US-Ha1 site (Fig. 1e). The LAI_e measurements at CA-SOA site in 1997 were less intensive than those at US-Ha1 site (Fig. 1a). However, the seasonal trajectory of leaf growth and almost unchanged peak of overstory LAI were also well captured at CA-SOA site (Fig. 1a). Compared to the intensive LAI_e measurements at deciduous broadleaf forest sites, the LAI_e measurements at evergreen conifer sites were much sparser (Fig. 1b–d and f–h). The overstory canopy of those evergreen conifer forest sites (Fig. 1b–d and f–h) were more clumped (lower Ω) than that of the two deciduous broadleaf forest sites (Fig. 1a and e). The summer LAI of overstory canopy at boreal forest sites (Fig. 1a–d) were lower than those of temperate forest sites (Fig. 1e–h).

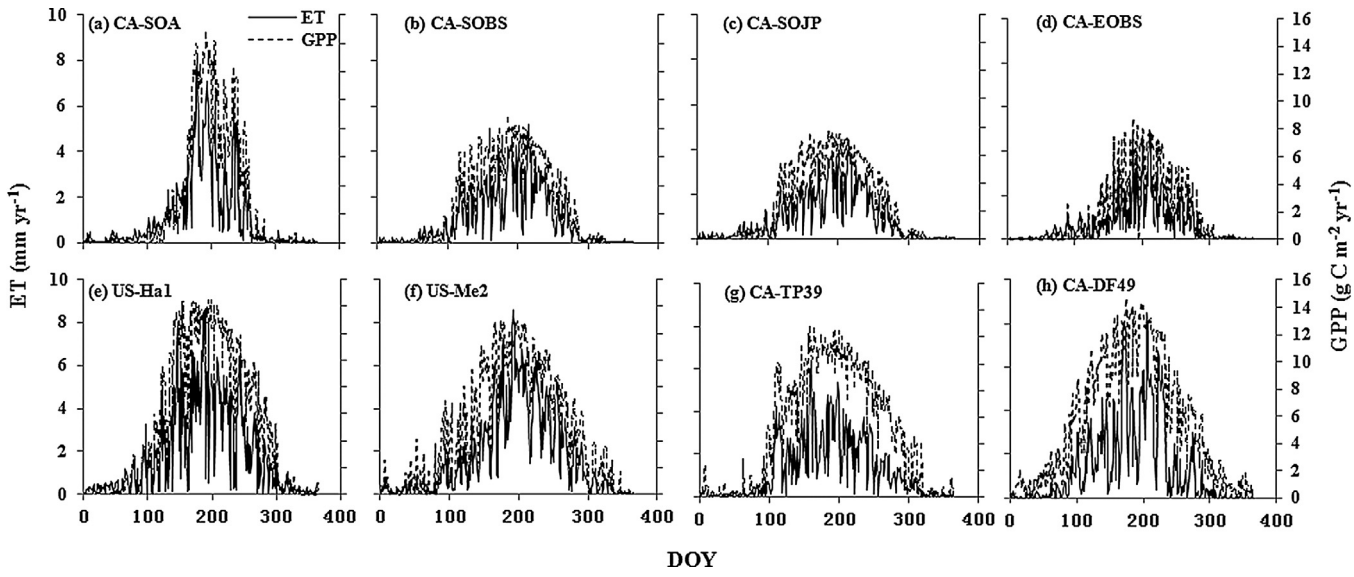

Fig. 2. Daily BEPS modeled ET and GPP across a year for each site. (a) CA-SOA site in 2002; (b) CA-SOBS site in 2001; (c) CA-SOJP site in 2001; (d) CA-EOBS site in 2004; (e) US-Ha1 site in 2010; (f) US-Me2 site in 2002; (g) CA-TP39 site in 2008; (h) CA-DF49 site in 2004.

3.2. Daily modeled GPP and ET from BEPS simulations

The gross primary productivity (GPP) is referred as the gross CO_2 uptake by vegetation per unit ground surface area and time. In BEPS, leaf-level GPP or photosynthesis rate constrains the stomatal conductance through the BWB model (Eq. (7)). Fig. 2 shows seasonal variations of daily ET and GPP at the studied sites calculated from the half-hourly time series of BEPS simulation.

The boreal deciduous broadleaf forest (i.e. CA-SOA site) (Fig. 2a) had higher summer ET and GPP values than boreal evergreen conifer forests (Fig. 2b–d), although they had similar magnitude of summer LAI (Fig. 1a–d). This mainly results from the higher value of maximum carboxylation rate (V_{cmax}) used in BEPS for CA-SOA site than those of boreal evergreen conifer forest sites. The four temperate forest sites had similar magnitude of summer GPP (Fig. 2e–h) because the lower summer LAI at US-Ha1 site compared to the three temperate evergreen conifer forest sites (Fig. 2f–h) were offset by other factors (i.e. V_{cmax}, meteorological variables and soil moisture). The summer ET at CA-TP39 site was lower than from the other three temperate forest sites (Fig. 2e–h) because it is sandy soil (98% sand) at CA-TP39 site. The sandy soil has a very low field capacity and cannot retain sufficient soil moisture to supply the white pine roots with enough water to meet the high transpiration demand of the canopy. This soil water stress on the stomatal conductance is well described using the model parameter (f_W) in BEPS (Ju et al., 2006).

The half-hourly GPP and ET simulations were compared with EC measurements to evaluate the performance of BEPS in predicting GPP and ET at all studied sites (Table 3). The regression statistics are summarized in Table 3. The root mean square error (RMSE) of simulated GPP ranges from 2.02 to 4.47 μmol m^{-2} s^{-1} and that of ET ranges from 0.02 to 0.05 mm h h^{-1}. BEPS is able to explain 56–88% of the variance of GPP and 43–75% of the variance of ET (Table 3). The RMSE and R^2 values indicated that the BEPS model can generally capture the half-hourly variability at most of the sites.

The BEPS modeled annual ET and GPP values were calculated from the daily sums, and their relationship with summer overstory LAI from studied sites are shown in Fig. 3. Both annual ET and GPP were positively related to the summer overstory LAI for the six evergreen conifer forest sites (Fig. 3). The summer overstory LAI usually represents the maximum LAI in the overstory canopy and is significantly and positively correlated with annual GPP (R^2 = 0.85), denoting the large contribution of summer GPP to annual G Likewise, the summer overstory LAI accounted for most of the surface area used in site-level ET calculations in summer, which contributes to most of the annual ET, and results in positively correlations between summer peak LAI and annual ET (R^2 = 0.55).

3.3. Impacts of foliage clumping on the simulations of ET components

Table 4 summarizes the ET results from the three simulation experiments at the studied sites. The site-averaged mean annual transpiration rate of the overstory canopy (T_o) was the largest ET component. T_o for the shaded leaves was slightly higher than that for the sunlit leaves, majorly resulting from higher shaded LAI than sunlit LAI in overstory canopy at the studied sites. For the same reason, the evaporation from the shaded portion of overstory canopy is higher than that from the sunlit portion (Table 4).

On the basis of Case I, where foliage clumping is considered and LAI is used, the effect of clumping on the estimation of site-averaged mean annual overstory canopy transpiration (T_o) is evaluated (Table 4). With a mean clumping index of 0.6 from all the sites (Table 1), the site-averaged T_o for Case II (clumping not considered and LAI used) is 5% higher than that for Case I (clumping

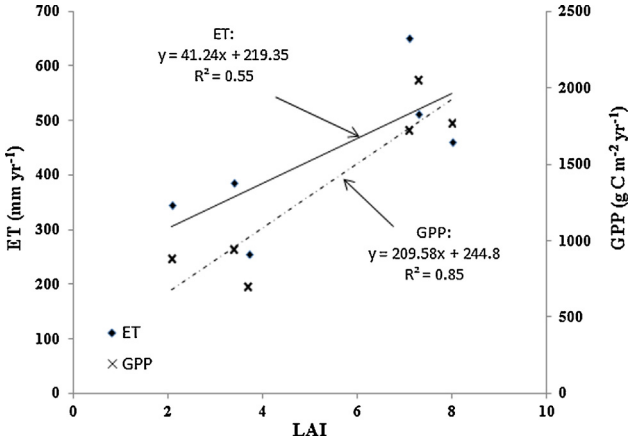

Fig. 3. Annual BEPS modeled ET and GPP against summer maximum LAI of the overstory canopy in a representative year for the six evergreen conifer forest sites.

Table 3
Intercepts (a), slopes (b), coefficients of determination (R^2), root mean square of errors (RMSE) from regressions of half-hourly GPP and ET fluxes by the BEPS model vs. half-hourly GPP and ET fluxes measured by EC in the fetch area of the flux towers of the studied sites.

Site ID	Period	Climate zone	Veg. type	Clumping Index	*a*		*b*		R^2		RMSE		*n*	
					GPP (μmol m^{-2} s^{-1})	ET (mm h^{-1})	GPP	ET	GPP	ET	GPP (μmol m^{-2} s^{-1})	ET (mm h^{-1})	GPP	ET
CA-SOA	2002–2010	Boreal	DBF	0.870	0.16	0.004	1.03	1.01	0.86	0.75	2.68	0.03	146,821	137,712
US-Ha1[a]	1992–2012	Temperate	DBF	0.70[c]	0.44	0.005	0.99	1.01	0.88	0.75	2.99	0.03	184,080	100,143
CA-SOBS	2001–2008	Boreal	ENF	0.660	0.19	0.004	1.00	0.96	0.79	0.66	2.02	0.02	137,355	122,047
CA-SOJP	2000–2009	Boreal	ENF	0.600	0.82	0.005	1.03	0.85	0.56	0.55	3.14	0.02	95,068	153,504
CA-EOBS	2004–2009	Boreal	ENF	0.586	0.29	0.001	1.07	0.91	0.70	0.61	2.40	0.02	101,166	105,216
CA-TP39	2008–2010	Temperate	ENF	0.513	0.46	0.001	1.06	0.91	0.86	0.69	3.12	0.03	52,608	52,608
US-Me2	2002–2008	Temperate	ENF	0.51[c]	0.07	0.006	1.07	1.04	0.66	0.43	4.47	0.05	122,024	122,736
CA-DF49	2000–2006	Temperate	ENF	0.488	–0.11	0.000	0.94	1.19	0.82	0.48	3.54	0.04	121,081	116,533

[a] Hourly data for this site.

considered and LAI used). This result is due to the overestimation of LAI_{sun} and the underestimation of LAI_{shade} in Case II. As T_{sun} per leaf area is usually larger than T_{shade}, the total T_o can be overestimated (Eq. (8)). Opposite to Case II, ignoring clumping in Case III (clumping not considered and LAI_e used) results in 15% underestimation of the total T_o. This is because the LAI_e is much smaller than the LAI for a highly clumped canopy. When the LAI_e is used without considering the clumping, LAI_{sun} is the same as that in Case I while LAI_{shade} is smaller than that in Case I. T_{shade} in Case III are therefore smaller than those in Case I while T_{sun} in Case III are nearly the same as those in Case I, resulting in an overall underestimate of T_o (Table 4).

Total evaporation (E_o) from the overstory canopy is almost the same for these three simulation cases, as the magnitude of evaporation from overstory canopy intercepted water is much smaller than that of overstory canopy transpiration (Table 4). Total understory T (T_u) for Case II is almost the same as that of Case I while T_u for Case III is lower than that of Case I as the shaded T_u in Case III is lower than that of Case I (Table 4). The absolute values of understory evaporation E_u is very small (Table 4) and the foliage clumping effects on the E_u estimation is not discussed here. Total evaporation from the ground surface (ES) in Case II is 2% lower than that in Case I (Table 4) as the net shortwave radiation of the ground is underestimated (Eqs. (A6) and (A9)) in Case II in which the correct LAI is used without considering the clumping effect. Ignoring clumping (in Case III) results in 6% overestimation of ES (Table 4) as the LAI_e is much smaller than the LAI for a clumped canopy and the net radiation of the ground is overestimated (Eqs. (A6), (A9) and (A17)).

The correlation of the bias errors in ET due to ignoring clumping and the clumping index is shown in Fig. 4. The bias error in ET due to ignoring clumping when the accurate LAI is used (Case II–Case I) is negatively related to the clumping index (Fig. 4a), whereas, the bias error in ET due to ignoring clumping when LAI_e is used (Case III–Case I) is positively related to the clumping index (Fig. 4b). This indicates that the more clumped of the canopy, the larger bias error in ET estimation due to ignoring foliage clumping.

3.4. The influence of foliage clumping on the calculation of key meteorological and ecosystem variables

The previous findings have illustrated the foliage clumping effects on ET components and total ET among studied sites. Now, we explore the foliage clumping effects on the key meteorological and ecosystem variables controlling ET estimation. The impacts of foliage clumping on the calculations of key meteorological and ecosystem variables (i.e. PPFD, net radiation, LAI, stomatal conductance and transpiration rates) according to sunlit or shaded leaves are investigated in Figs. 5 and 6.

If the LAI is used in ET estimation (ignoring the foliage clumping), absorbed PPFD, R_n and transpiration rate of the sunlit representative leaf will be negatively biased with clumping index. In contrast, the shaded representative leaf will be positively biased with clumping index (Fig. 5a, b and e). For example, for a typical boreal conifer forest, where LAI is 4.0 and Ω is 0.5, downward shortwave radiation above canopy is 500 W m^{-2} and relative humidity is 50%, PPFD, R_n and respiration rate of the shaded representative leaf at $\theta = 45^\circ$ are 127.23 μmol m^{-2} s^{-1}, 13.59 W m^{-2} and 0.0042 g H_2O m^{-2} s^{-1}, respectively, without considering clumping. However, they will be 99.99 μmol m^{-2} s^{-1}, 10.36 W m^{-2} and 0.0033 g H_2O m^{-2} s^{-1}, respectively, when the clumping is considered (Fig. 5a, b and e). The PPFD, R_n and transpiration rate of the sunlit representative leaf will be 597.44 μmol m^{-2} s^{-1}, 138.93 W m^{-2} and 0.0414 g H_2O m^{-2} s^{-1}, respectively, without considering clumping, but they will be 623.06 μmol m^{-2} s^{-1}, 152.53 W m^{-2} and 0.0455 g H_2O m^{-2} s^{-1}, respectively, when the clumping is considered (Fig. 5a, b and e). In this case, the relative error in PPFD, R_n and transpiration rate estimation when clumping is ignored will be 27%, 31% and 27%,

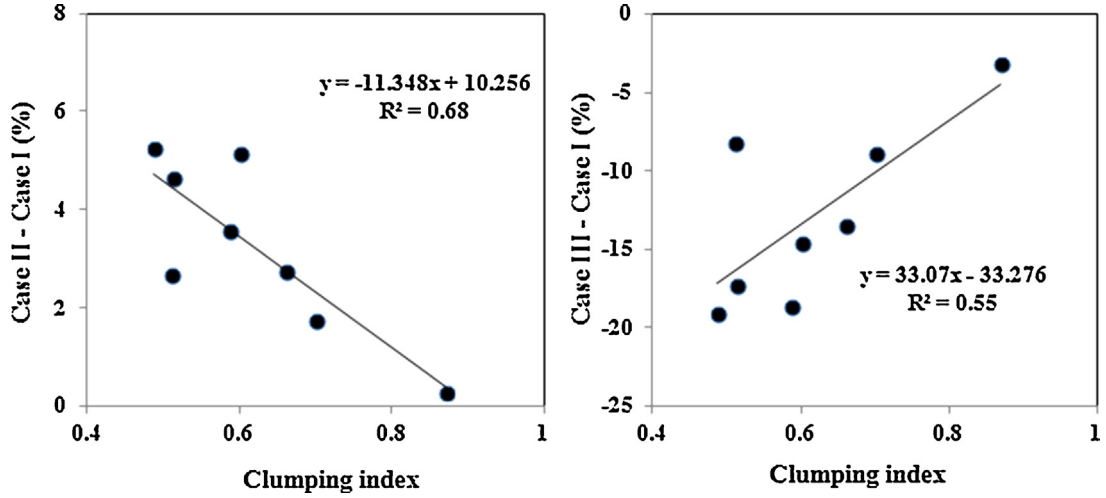

Fig. 4. The regression of bias error in ET due to ignoring clumping when accurate LAI is used (Case II–Case I) or when LAI_e is used (Case III–Case I) against the clumping index.

Table 4
ET components (mm yr^{-1}) at the studied sites under three canopy architectural treatments.

ET		T_o	E_o	T_u	E_u	ES	ET_tot
Sunlit portion	Case I	117.3 (±46.9)	13.0 (±5.1)	20.4 (±22.0)	3.5 (±3.5)		
	Case II	126.9 (±47.5)	14.0 (±5.4)	20.0 (±21.1)	4.0 (±3.5)		
	Case III	122.6 (±47.0)	13.8 (±5.5)	23.0 (±21.3)	4.0 (±3.4)		
Shaded portion	Case I	176.7 (±87.8)	51.8 (±41.4)	15.0 (±14.1)	5.1 (±5.0)		
	Case II	182.1 (±93.5)	51.0 (±41.5)	12.1 (±13.9)	4.6 (±5.0)		
	Case III	128.1 (±65.6)	33.3 (±26.1)	10.4 (±12.3)	3.9 (±4.2)		
Total	Case I	294.0 (±126.1)	64.8 (±45.4)	35.4 (±35.9)	8.7 (±8.5)	42.1 (±20.2)	444.9 (±151.5)
	Case II	309.1 (±131.7)	65.0 (±45.6)	32.1 (±34.5)	8.6 (±8.5)	41.1 (±19.2)	455.9 (±156.6)
	Case III	250.7 (±107.6)	47.1 (±30.8)	33.3 (±33.5)	7.9 (±7.5)	44.6 (±19.6)	383.7 (±132.4)
Case II–Case I		15.1 (5.1%)	0.2 (0.2%)	−3.3 (−9.3%)	−0.1 (−1.0%)	−0.9 (−2.2%)	10.9 (2.5%)
Case III–Case I		−43.3 (−14.7%)	−17.8 (−27.4%)	−2.0 (−5.8%)	−0.8 (−9.3%)	2.6 (6.2%)	−61.3 (−13.8%)

T_o: transpiration rate from the overstory, E_o: evaporation rate from the overstory, T_u: transpiration rate from the understory, E_u: evaporation rate from the understory, ES: evaporation rate from the ground surface, ET_tot: total ET. Based on double-tailed t-test, the differences between Case I and Case II and between Case I and Case III for each ET component and the total ET are all statistically highly significant ($p < 0.001$).

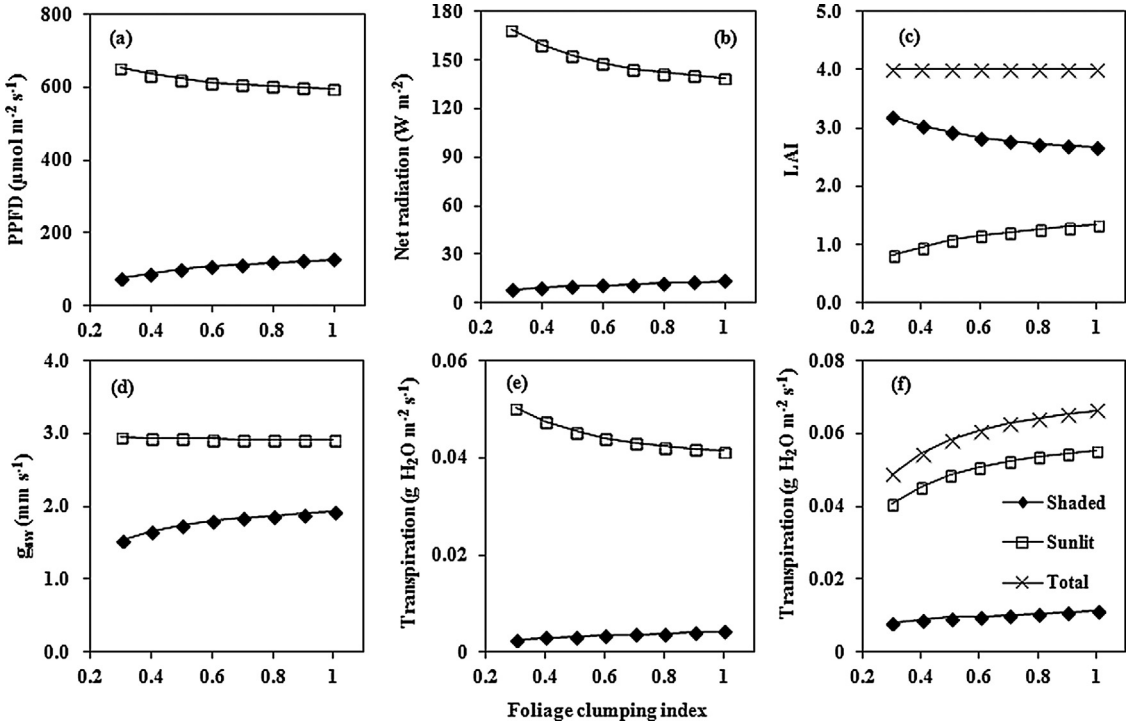

Fig. 5. Variation of (a) absorbed photosynthetic photon flux density (PPFD), (b) net radiation, (c) LAI, (d) stomatal conductance, (e) leaf-level transpiration rates, (f) canopy-level transpiration rates for sunlit and shaded leaf or canopy, with clumping index, when the LAI is used ignoring clumping (Case II), solar zenith angle, $\theta = 45^\circ$, air temperature = 15 °C, relative humidity = 50%, aerodynamic resistance = 5 s m^{-1}, downward shortwave radiation above canopy = 500 W m^{-2}.

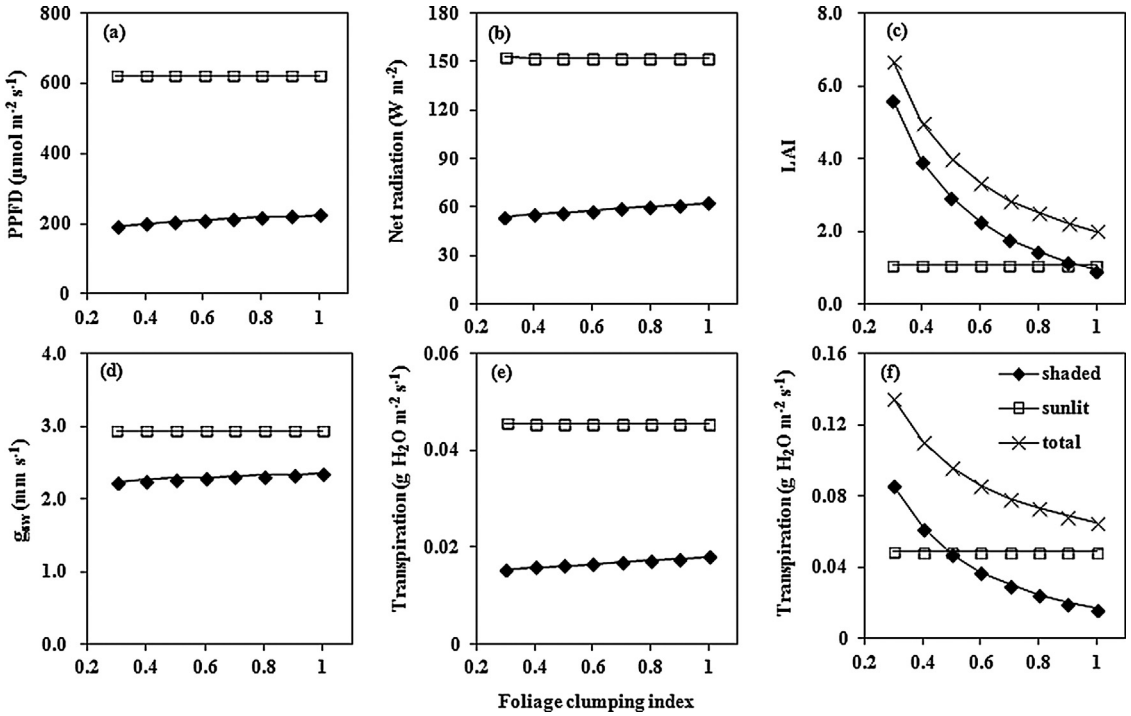

Fig. 6. Variation of (a) PPFD, (b) net radiation, (c) LAI, (d) stomatal conductance, (e) leaf-level transpiration rates, (f) canopy-level transpiration rates for sunlit and shaded leaf or canopy, with clumping index, when the LAIe (LAI_e) = 2.0 (Case III), solar zenith angle = 45°, air temperature = 15 °C, relative humidity = 50%, aerodynamic resistance = 5 s m^{-1}, downward shortwave radiation above canopy = 500 W m^{-2}.

respectively, for the shaded representative leaf and they will be −4%, −9% and −9%, respectively, for the sunlit representative leaf. In this case, the sunlit LAI will be overestimated by 24% while the shaded LAI will be underestimated by 9% (Fig. 5c). The stomatal conductance (g_{sw}) of the sunlit representative leaf is almost invariant while that of the shaded representative leaf is positively biased by 10% in this case (Fig. 5d). The shaded portion, the sunlit portion and the total canopy ET were overestimated by 18%, 13% and 14%, respectively, when the clumping is ignored in this case (Fig. 5f).

Nadir-view optical multi-spectral remote sensing signals contain information on the LAIe rather than the actual LAI. As the clumping index decreases (more clumped) at the same LAIe, the shaded LAI and the total LAI increase. If the LAI_e is used in the ET estimation, ignoring the foliage clumping (Case III), absorbed PPFD, R_n, g_{sw} and transpiration rate of the sunlit representative leaf will be invariant with clumping index while those for the shaded representative leaf will be positively biased with clumping index (Fig. 6a, b, d and e).

Using the same example as in Fig. 6 (i.e. L_e = 2.0, Ω = 0.5), PPFD, R_n, g_{sw} and transpiration rate of the shaded representative leaf at θ = 45° will be 224.82 μmol m^{-2} s^{-1}, 62.67 W m^{-2}, 2.35 mm s^{-1} and 0.018 g H_2O m^{-2} s^{-1}, respectively, without considering clumping, but they will be 205.55 μmol m^{-2} s^{-1}, 56.75 W m^{-2}, 2.28 mm s^{-1} and 0.016 g H_2O m^{-2} s^{-1}, respectively, when the clumping is considered (Fig. 6a, b, d and e). In this case, the relative error in PPFD, R_n, g_{sw} and transpiration rate estimation when clumping is ignored will be 9%, 10%, 3% and 13%, respectively, for the shaded representative leaf. In this case, sunlit LAI is invariant while shaded LAI and total LAI will be underestimated by 68% and 50%, respectively, when the clumping is ignored (Fig. 6c). The shaded portion and the total canopy T will be underestimated by 65% and 32% when the clumping is ignored in this case (Fig. 6f).

3.5. Sensitivity test of ET simulation to errors in input and model parameters

Uncertainties in the ET simulation due to errors in input and model parameters may be as large as the clumping effects reported above. To explore the reliability of our conclusions about the clumping effects, we conducted a set of sensitivity tests for two key canopy structural parameters (LAI and Ω) and two key ecophysiological parameters (f_w and V_{cmax}) (Table 5).

When the LAI in each site is increased or decreased by 20%, the site-averaged mean annual total ET is increased or decreased by about 8%. However, the relative differences between Case I and Case II and between Case I and Case III are less than 1% with these LAI changes, suggesting that an LAI change would affect all cases in the same direction (ET in the three cases all become larger or smaller). Similarly, forcing the soil water scalar (f_w) and maximum rate of carboxylation (V_{cmax}) to increase or decrease by 20% in the model would result in increase or decrease of site-averaged mean annual total ET in similar magnitudes, while the relative differences between the cases quantifying the clumping effects are affected very little. In general, modifying other parameters such as maximum rate of electron transport (J_{max}) and the slope in the BWB equation (m) would move all of the three cases in the same direction, and the clumping effects quantified as the relative differences in site-averaged mean annual ET between cases would not be much affected by these modifications. This set of sensitivity analysis indicates the spatially consistent clumping effects and supports the levels of their statistical significance.

Increasing or decreasing the Ω value by 20% did not considerably affect the clumping effects quantified as the relative difference in ET among the cases in this study (Table 5). In the preliminary evaluation using the existing ground data, the mean bias error of Ω is less than 10% (5% error in needle-to-shoot ratio and 5% error in element clumping index) (Chen et al., 2006). Thus, the 20% change

Table 5
Sensitivity of site-averaged ET ($mm\,yr^{-1}$) to errors in the major input parameters of leaf area index (LAI) and Ω (Ω), maximum rate of carboxylation (V_{cmax}) as well as the most uncertain soil water scalar (f_w) for stomatal conductance.

	Case I	Case II	Case III	Case II–Case I	Case III–Case I
Baseline	445	456	384	11 (2.5%)	−61 (−13.8%)
1.2 × LAI	480 (7.9%)	491	413	11 (2.2%)	−67 (−14.0%)
0.8 × LAI	406 (−8.7%)	417	352	10 (2.5%)	−54 (−13.2%)
1.2 × f_w	483 (8.6%)	497	421	14 (2.8%)	−63 (−13.0%)
0.8 × f_w	405 (−9.0%)	413	345	8 (2.0%)	−60 (−14.8%)
1.2 × Ω	449 (1.0%)	461	388	12 (2.6%)	−62 (−13.7%)
0.8 × Ω	439 (−1.3%)	450	379	11 (2.4%)	−60 (−13.7%)
1.2 × V_{cmax}	459 (3.2%)	471	399	12 (2.7%)	−60 (−13.1%)
0.8 × V_{cmax}	428 (−3.9%)	437	365	9 (2.2%)	−63 (−14.7%)

The percentage in the brackets of the second column is the difference relative to the baseline.
The percentage in the brackets of the last two columns is the difference relative to Case I.
The baseline represents the ideal case shown in Table 4.

in Ω is large enough for most of the vegetation types. Although Ω is decreased or increased by 20%, we still have 3% difference between Case II and Case I and 14% difference between Case III and Case I which were the same as the baseline simulation in this study (Table 5).

4. Conclusions

We used an ecosystem model (BEPS) to assess the effects of foliage clumping, characterized by the clumping index (Ω), on the estimation of ET in forests. BEPS contains a comprehensive description of canopy radiation transfer in a two-leaf (sunlit/shaded) scheme and couples water and carbon simulations tightly. The performance of BEPS in estimating ET and GPP was first assessed by comparing the simulated ET and GPP with the measurements from 8 North American EC flux tower sites. BEPS can explain 43–75% and 56–88% variance of measured ET and GPP at these sites, respectively. Three cases are simulated: (1) LAI and Ω are considered, (2) the LAI is considered but Ω is ignored (assuming to be one), and (3) the LAI is replaced with the effective LAI and Ω is assumed to be one. The importance of foliage clumping to ET estimation is illustrated from its impacts on LAI derivation from the effective LAI, on sunlit and shaded LAI stratification, and on leaf-level radiation calculations. The major conclusions are drawn as follows:

1. Even if we have accurate LAI values for a site, ignoring foliage clumping would result in overestimation of site-level ET. This bias is found to increase with clumping (or decrease with clumping index). The bias is the highest (~5%) for the conifer forests and correlated closely with the variation in the clumping index ($r^2 = 0.68$).
2. When the LAI is replaced with the effective LAI (LAI_e), ET is underestimated at all sites tested. With a mean clumping index of 0.6 for these sites, the mean annual ET is underestimated by 11.5% on average at these sites. For the most clumped site, the mean annual ET is underestimated by 19.1%. In general, the more clumped a canopy is, the larger bias error is in ET estimation due to ignoring foliage clumping ($r^2 = 0.55$).
3. Although there are still some uncertainties in site-level ET simulation due to errors in input and model parameters, the foliage clumping effects quantified as the relative differences in site-averaged mean annual ET between the cases with and without the clumping consideration are still robust because errors in input and model parameters would move all cases in the same directions.
4. Our results suggest the need for considering foliage clumping in ET estimation. In particular, when LAI is derived from optical measurements on the ground and from satellite platforms without considering the effect of clumping, it can cause substantial underestimation of ET.

Acknowledgements

The authors wish to thank Alan Barr, Andy Black, Harry McCaughey, David R. Foster, Hank Margolis, Altaf Arain and Beverly Law for their leading work at those flux tower sites of Canadian Carbon Program (ftp://daac.ornl.gov/data/fluxnet/private/fluxnet_canada/e_about.htm) and Ameriflux (http://ameriflux.ornl.gov/). This research is supported by National Natural Science Foundation of China (Grant number: 41503070) and the Canadian Space Agency (CSA) (Grant number: 14SUSMAPTO).

Appendix A. Algorithms for net radiation of vegetation and ground surface

The hourly BEPS model calculates the net radiation of the sunlit and shaded representative leaf for the overstory and understory canopy separately:

$$R^*_{sun\_o} = S^*_{dir\_o} + S^*_{dif\_o}/LAI_o + L^*_o/LAI_o \quad (A1a)$$

$$R^*_{shade\_o} = S^*_{dif\_o}/LAI_o + L^*_o/LAI_o \quad (A1b)$$

$$R^*_{sun\_u} = S^*_{dir\_u} + S^*_{dif\_u}/LAI_u + L^*_u/LAI_u \quad (A1c)$$

$$R^*_{shade\_u} = S^*_{dif\_u}/LAI_u + L^*_u/LAI_u \quad (A1d)$$

where the capital symbols of S and L denote shortwave and longwave irradiances, respectively; superscript asterisk denotes the net radiation component and the subscripts 'sun' and 'shade' denote the sunlit and shaded representative leaf, respectively. The subscripts 'o' and 'u' denote overstory and understory, respectively. The subscripts 'dir' and 'dif' denote direct and diffuse components. Downward fluxes are defined as positive conventionally. The calculation of the shortwave radiation components are based on Chen et al. (1999). The partition of global incoming solar radiation into direct and diffuse components is done using the following equations:

$$\frac{S_{dif}}{S_g} = \begin{cases} 0.943 + 0.734r - 4.9r^2 + 1.796r^3 + 2.058r^4 & r < 0.8 \\ 0.13 & r \geq 0.8 \end{cases} \quad (A2a)$$

$$S_{dir} = S_g - S_{dif} \quad (A2b)$$

where S_g is the incoming global solar radiation in $W\,m^{-2}$, the parameter r is defined as:

$$r = \frac{S_g}{S_0 \cos\theta} \quad (A3)$$

where S_0 and θ are the solar constant (=1367 $W\,m^{-2}$) and solar zenith angle, respectively.

The direct component of net shortwave radiation of the sunlit representative leaf in the overstory canopy is calculated as:

$$S^*_{\mathrm{dir\_o}} = (1-\alpha_o)S_{\mathrm{dir}}\cos\alpha/\cos\theta \tag{A4}$$

and the direct component of net shortwave radiation of the sunlit representative leaf in the understory canopy is calculated as:

$$S^*_{\mathrm{dir}_u} = \frac{(1-\alpha_u)S_{\mathrm{dir}}\cos\alpha}{\cos\theta} \tag{A5}$$

and the direct component of net shortwave radiation of the ground is calculated as:

$$S^*_{\mathrm{dir\_g}} = (1-\alpha_{\mathrm{g}})S_{\mathrm{dir}}\mathrm{e}^{-0.5\Omega(\mathrm{LAI_o}+\mathrm{LAI_u})/\cos\theta} \tag{A6}$$

where α_{o}, α_{u} and α_{g} are the albedo of the overstory canopy, understory canopy and the ground surface, respectively. α is mean leaf-sun angle. $\alpha = 60^\circ$ for a canopy with spherical leaf angle distribution (Chen, 1996b).

Similarly, the diffuse component of net shortwave radiation of overstory canopy, understory canopy and the ground surface are calculated as:

$$S^*_{\mathrm{dif\_o}} = S_{\mathrm{dif}}[(1-\alpha_{\mathrm{o}}) - (1-\alpha_{\mathrm{u}})\mathrm{e}^{-0.5\Omega\mathrm{LAI_o}/\cos\bar{\theta}_{\mathrm{o}}}] + C_{\mathrm{o}}\mathrm{LAI_o} \tag{A7}$$

$$S^*_{\mathrm{dif\_u}} = [(1-\alpha_{\mathrm{u}}) - (1-\alpha_{\mathrm{g}})\mathrm{e}^{-0.5\Omega\mathrm{LAI_u}/\cos\bar{\theta}_{\mathrm{u}}}]S_{\mathrm{dif}}\mathrm{e}^{-0.5\Omega\mathrm{LAI_o}/\cos\bar{\theta}_{\mathrm{o}}} + C_{\mathrm{u}}\mathrm{LAI_u} \tag{A8}$$

$$S^*_{\mathrm{dif\_g}} = (1-\alpha_{\mathrm{g}})S_{\mathrm{dif}}\mathrm{e}^{-0.5\Omega\mathrm{LAI_o}/\cos\bar{\theta}_{\mathrm{o}} - 0.5\Omega\mathrm{LAI_u}/\cos\bar{\theta}_{\mathrm{u}}} \tag{A9}$$

C arises from multiple scattering of direct radiation. The equations for calculating C is derived based on (Norman, 1982) with a modification by Chen et al. (1999):

$$C_{\mathrm{o}} = 0.07\Omega S_{\mathrm{dir}}(1.1 - 0.1\mathrm{LAI_o})\mathrm{e}^{-\cos\theta} \tag{A10}$$

$$C_{\mathrm{u}} = 0.07\Omega S_{\mathrm{dir}}\mathrm{e}^{-0.5\Omega\mathrm{LAI_o}/\cos\theta}(1.1 - 0.1\mathrm{LAI_u})\mathrm{e}^{-\cos\theta} \tag{A11}$$

$\bar{\theta}$ is a representative zenith angle for diffuse radiation transmission and slightly dependent on LAI:

$$\cos\bar{\theta} = 0.537 + 0.025\mathrm{LAI} \tag{A12}$$

This is a simple but an effective way to calculate the transmitted diffuse radiation. It avoids the integration of the sky irradiance for the hemisphere by using a representative transmission zenith angle $\bar{\theta}$, which is obtained through a numerical experiment with the complete integration. Under the assumption of isotropic sky radiance distribution, it is near a constant of 57.5°, but also a weak function of LAI. This angle is larger than the mean of 45° because the hemisphere is more heavily weighted against the lower sphere in the integration. The dependence on LAI is found because it modifies slightly the weight distribution (Liu et al., 2003).

For the ground surface underneath the vegetation, net radiation is:

$$R^*_{\mathrm{g}} = S^*_{\mathrm{g}} + L^*_{\mathrm{g}} \tag{A13}$$

where the net shortwave radiation of the ground (S^*_{g}) are the sum of direct and diffuse components:

$$S^*_{\mathrm{g}} = S^*_{\mathrm{dir\_g}} + S^*_{\mathrm{dif\_g}} \tag{A14}$$

The net longwave radiation for the overstory canopy (L^*_{o}), understory canopy (L^*_{u}) and the ground surface (L^*_{g}) are calculated using the following equations:

$$\begin{aligned} L^*_{\mathrm{o}} = {} & \{\varepsilon_{\mathrm{o}}[\varepsilon_{\mathrm{a}}\sigma T_{\mathrm{a}}^4 + \varepsilon_{\mathrm{u}}\sigma T_{\mathrm{u}}^4(1-\mathrm{e}^{-0.5\mathrm{LAI_u}\Omega/\cos\bar{\theta}_{\mathrm{u}}})\varepsilon_{\mathrm{g}}\sigma T_{\mathrm{g}}^4\mathrm{e}^{-0.5\mathrm{LAI_u}\Omega/\cos\bar{\theta}_{\mathrm{u}}}] \\ & - 2\varepsilon_0\sigma T_{\mathrm{o}}^4\}(1-\mathrm{e}^{-0.5\mathrm{LAI_o}\Omega/\cos\bar{\theta}_{\mathrm{o}}}) + \varepsilon_{\mathrm{o}}(1-\varepsilon_{\mathrm{u}}) \\ & (1-\mathrm{e}^{-0.5\mathrm{LAI_u}\Omega/\cos\bar{\theta}_{\mathrm{u}}})[\varepsilon_{\mathrm{a}}\sigma T_{\mathrm{a}}^4\mathrm{e}^{-0.5\mathrm{LAI_o}\Omega/\cos\bar{\theta}_{\mathrm{o}}} \\ & + \varepsilon_0\sigma T_{\mathrm{o}}^4(1-\mathrm{e}^{-0.5\mathrm{LAI_o}\Omega/\cos\bar{\theta}_{\mathrm{o}}})] \end{aligned} \tag{A15}$$

$$\begin{aligned} L^*_{\mathrm{u}} = {} & \{\varepsilon_{\mathrm{u}}[\varepsilon_{\mathrm{a}}\sigma T_{\mathrm{a}}^4\mathrm{e}^{-0.5\mathrm{LAI_o}\Omega/\cos\bar{\theta}_{\mathrm{o}}} + \varepsilon_{\mathrm{o}}\sigma T_{\mathrm{o}}^4(1-\mathrm{e}^{-0.5\mathrm{LAI_o}\Omega/\cos\bar{\theta}_{\mathrm{o}}}) \\ & + \varepsilon_{\mathrm{g}}\sigma T_{\mathrm{g}}^4] - 2\varepsilon_{\mathrm{u}}\sigma T_{\mathrm{u}}^4\}(1-\mathrm{e}^{-0.5\mathrm{LAI_u}\Omega/\cos\bar{\theta}_u}) \\ & + \varepsilon_{\mathrm{u}}(1-\varepsilon_{\mathrm{g}})\{[\varepsilon_{\mathrm{a}}\sigma T_{\mathrm{a}}^4\mathrm{e}^{-0.5\mathrm{LAI_o}\Omega/\cos\bar{\theta}_{\mathrm{o}}} \\ & + \varepsilon_{\mathrm{o}}\sigma T_{\mathrm{o}}^4(1-\mathrm{e}^{-0.5\mathrm{LAI_o}\Omega/\cos\bar{\theta}_{\mathrm{o}}})]\mathrm{e}^{-0.5\mathrm{LAI_u}\Omega/\cos\bar{\theta}_{\mathrm{u}}} \\ & + \varepsilon_{\mathrm{u}}\sigma T_{\mathrm{u}}^4(1-\mathrm{e}^{-0.5\mathrm{LAI_u}\Omega/\cos\bar{\theta}_{\mathrm{u}}})\} \\ & + \varepsilon_{\mathrm{u}}(1-\varepsilon_0)[\varepsilon_{\mathrm{u}}\sigma T_{\mathrm{u}}^4(1-\mathrm{e}^{-0.5\mathrm{LAI_u}\Omega/\cos\bar{\theta}_{\mathrm{u}}}) \\ & + \varepsilon_{\mathrm{g}}\sigma T_{\mathrm{g}}^4\mathrm{e}^{-0.5\mathrm{LAI_u}\Omega/\cos\bar{\theta}_{\mathrm{u}}})](1-\mathrm{e}^{-0.5\mathrm{LAI_o}\Omega/\cos\bar{\theta}_{\mathrm{o}}}) \end{aligned} \tag{A16}$$

$$\begin{aligned} L^*_{\mathrm{g}} = {} & \varepsilon_{\mathrm{g}}\{[\varepsilon_{\mathrm{a}}\sigma T_{\mathrm{a}}^4\mathrm{e}^{-0.5\mathrm{LAI_o}\Omega/\cos\bar{\theta}_{\mathrm{o}}} \\ & + \varepsilon_{\mathrm{o}}\sigma T_{\mathrm{o}}^4(1-\mathrm{e}^{-0.5\mathrm{LAI_o}\Omega/\cos\bar{\theta}_{\mathrm{o}}})]\mathrm{e}^{-0.5\mathrm{LAI_u}\Omega/\cos\bar{\theta}_{\mathrm{u}}} \\ & + \varepsilon_{\mathrm{u}}\sigma T_{\mathrm{u}}^4(1-\mathrm{e}^{-0.5\mathrm{LAI_u}\Omega/\cos\bar{\theta}_{\mathrm{u}}})\} - \varepsilon_{\mathrm{g}}\sigma T_{\mathrm{g}}^4 \\ & + \varepsilon_{\mathrm{g}}(1-\varepsilon_{\mathrm{u}})\langle\varepsilon_{\mathrm{g}}\sigma T_{\mathrm{g}}^4 + (1-\varepsilon_{\mathrm{g}})\{[\varepsilon_{\mathrm{a}}\sigma T_{\mathrm{a}}^4\mathrm{e}^{-0.5\mathrm{LAI_o}\Omega/\cos\bar{\theta}_{\mathrm{o}}} \\ & + \varepsilon_{\mathrm{o}}\sigma T_{\mathrm{o}}^4 1-\mathrm{e}^{-0.5\mathrm{LAI_o}\Omega/\cos\bar{\theta}_{\mathrm{o}}})]\mathrm{e}^{-0.5\mathrm{LAI_u}\Omega/\cos\bar{\theta}_{\mathrm{u}}} \\ & + \varepsilon_{\mathrm{u}}\sigma T_{\mathrm{u}}^4(1-\mathrm{e}^{-0.5\mathrm{LAI_u}\Omega/\cos\bar{\theta}_{\mathrm{u}}})\}\rangle(1-\mathrm{e}^{-0.5\mathrm{LAI_u}\Omega/\cos\bar{\theta}_{\mathrm{u}}}) \end{aligned} \tag{A17}$$

where ε_{a}, ε_{o}, ε_{u} and ε_{g} are emissivities of the atmosphere, overstory, understory and ground surface, respectively. Prescribed values of 0.98, 0.98 and 0.95 are assigned to ε_{o}, ε_{u} and ε_{g}, respectively, according to (Chen and Zhang, 1989; Chen et al., 1989), and ε_{a} is compute as $\varepsilon_{\mathrm{a}} = 1.24\left(\frac{e_{\mathrm{a}}}{T_{\mathrm{a}}}\right)^{1/7}$ (Brutsaert, 1982), where e_{a} and T_{a} are water vapor pressure in mbar and temperature of the atmosphere in K. The representative angles for longwave transmission through the overstory and understory are treated the same as those for diffuse radiation transmission described in Eq. (A12). More terms were added into the previous equations (Liu et al., 2003) to consider the reflected longwave radiation from the neighbor layers.

References

Arain, M.A., Restrepo-Coupe, N., 2005. Net ecosystem production in a temperate pine plantation in southeastern Canada. Agric. For. Meteorol. 128 (3–4), 223–241.

Baldocchi, D., 1994. An analytical solution for coupled leaf photosynthesis and stomatal conductance models. Tree Physiol. 14 (7–8–9), 1069–1079, http://dx.doi.org/10.1093/treephys/14.7-8-9.1069.

Baldocchi, D.D., Vogel, C.A., Hall, B., 1997. Seasonal variation of carbon dioxide exchange rates above and below a boreal jack pine forest. Agric. For. Meteorol. 83 (1–2), 147–170, http://dx.doi.org/10.1016/S0168-1923(96)02335-0.

Ball, J.T., 1988. An Analysis of Stomatal Conductance. Stanford University, Stanford.

Band, L.E., Peterson, D.L., Running, S.W., Coughlan, J., Lammers, R., Dungan, J., Nemani, R., 1991. Forest ecosystem processes at the watershed scale: basis for distributed simulation. Ecol. Model. 56 (0), 171–196, http://dx.doi.org/10.1016/0304-3800(91)90199-B.

Barr, A.G., Black, T.A., Hogg, E.H., Kljun, N., Morgenstern, K., Nesic, Z., 2004. Inter-annual variability in the leaf area index of a boreal aspen-hazelnut forest in relation to net ecosystem production. Agric. For. Meteorol. 126 (3–4), 237–255.

Bergeron, O., Hank, A.M., Andrew, T., Carole, B., Allison, C.L., Alan, D.G., Steven, B.C.W., 2007. Comparison of carbon dioxide fluxes over three boreal black spruce forests in Canada. Glob. Change Biol. 13 (1), 89–107.

Black, T.A., Chen, J.-M., Lee, X., Sagar, R.M., 1991. Characteristics of shortwave and longwave irradiances under a Douglas-fir forest stand. Can. J. For. Res. 21 (7), 1020–1028, http://dx.doi.org/10.1139/x91-140.

Brutsaert, W., 1982. Evaporation into the Atmosphere. Springer, Netherlands, pp. 302, http://dx.doi.org/10.1007/978-94-017-1497-6.

Chen, B., Black, T.A., Coops, N.C., Krishnan, P., Jassal, R., Brummer, C., Nesic, Z., 2009. Seasonal controls on interannual variability in carbon dioxide exchange of a near-end-of rotation Douglas-fir stand in the Pacific Northwest, 1997–2006. Glob. Change Biol. 15 (8), 1962–1981.
Chen, B., Chen, J.M., Ju, W., 2007. Remote sensing-based ecosystem–atmosphere simulation scheme (EASS)—model formulation and test with multiple-year data. Ecol. Model. 209 (2), 277–300.
Chen, J.M., Black, T.A., 1991. Measuring leaf area index of plant canopies with branch architecture. Agric. For. Meteorol. 57 (1–3), 1–12, http://dx.doi.org/10.1016/0168-1923(91)90074-Z.
Chen, J.M., Black, T.A., 1992. Foliage area and architecture of plant canopies from sunfleck size distributions. Agric. For. Meteorol. 60 (3), 249–266.
Chen, J.M., Liu, J., Cihlar, J., Goulden, M.L., 1999. Daily canopy photosynthesis model through temporal and spatial scaling for remote sensing applications. Ecol. Model. 124 (2–3), 99–119.
Chen, J.M., Yang, B.J., Zhang, R.H., 1989. Soil thermal emissivity as affected by its water content and surface treatment. Soil Sci. 148 (6), 433–435.
Chen, J.M., Zhang, R.-H., 1989. Studies on the measurements of crop emissivity and sky temperature. Agric. For. Meteorol. 49 (1), 23–34, http://dx.doi.org/10.1016/0168-1923(89)90059-2.
Chen, J.M., 1996a. Optically-based methods for measuring seasonal variation of leaf area index in boreal conifer stands. Agric. For. Meteorol. 80 (2–4), 135–163, http://dx.doi.org/10.1016/0168-1923(95)02291-0.
Chen, J.M., 1996b. Canopy architecture and remote sensing of the fraction of photosynthetically active radiation absorbed by boreal conifer forests. IEEE Trans. Geosci. Remote Sens. 34 (6), 1353–1368.
Chen, J.M., Chen, X., Ju, W., Geng, X., 2005. Distributed hydrological model for mapping evapotranspiration using remote sensing inputs. J. Hydrol. 305 (1–4), 15–39, http://dx.doi.org/10.1016/j.jhydrol.2004.08.029.
Chen, J.M., Cihlar, J., 1995. Plant canopy gap-size analysis theory for improving optical measurements of leaf-arnea index. Appl. Opt. 34 (27), 6211–6222.
Chen, J.M., Govind, A., Sonnentag, O., Zhang, Y., Barr, A., Amiro, B., 2006. Leaf area index measurements at Fluxnet-Canada forest sites. Agric. For. Meteorol. 140 (1–4), 257–268, http://dx.doi.org/10.1016/j.agrformet.2006.08.005.
Chen, J.M., Mo, G., Pisek, J., Liu, J., Deng, F., Ishizawa, M., Chan, D., 2012. Effects of foliage clumping on the estimation of global terrestrial gross primary productivity. Glob. Biogeochem. Cycl. 26 (1), GB1019.
Collatz, G.J., Ball, J.T., Grivet, C., Berry, J.A., 1991. Physiological and environmental regulation of stomatal conductance, photosynthesis and transpiration: a model that includes a laminar boundary layer. Agric. For. Meteorol. 54 (2–4), 107–136.
Davidson, E.A., SAVAGE, K.E., TRUMBORE, S.E., BORKEN, W., 2006. Vertical partitioning of CO_2 production within a temperate forest soil. Glob. Change Biol. 12 (6), 944–956, http://dx.doi.org/10.1111/j.1365-2486.2005.01142.x.
Feng, X., Liu, G., Chen, J.M., Chen, M., Liu, J., Ju, W.M., . . . Zhou, W., 2007. Net primary productivity of China's terrestrial ecosystems from a process model driven by remote sensing. J. Environ. Manag. 85 (3), 563–573, http://dx.doi.org/10.1016/j.jenvman.2006.09.021.
Gonsamo, A., Chen, J.M., Price, D.T., Kurz, W.A., Liu, J., Boisvenue, C., . . . Chang, K.-H., 2013. Improved assessment of gross and net primary productivity of Canada's landmass. J. Geophys. Res.: Biogeosci. 118 (4), 1546–1560, http://dx.doi.org/10.1002/2013JG002388.
He, L., Chen, J.M., Pisek, J., Schaaf, C.B., Strahler, A.H., 2012. Global clumping index map derived from the MODIS BRDF product. Remote Sens. Environ. 119 (0), 118–130, http://dx.doi.org/10.1016/j.rse.2011.12.008.
Ju, W., Chen, J.M., Black, T.A., Barr, A.G., Liu, J., Chen, B., 2006. Modelling multi-year coupled carbon and water fluxes in a boreal aspen forest. Agric. For. Meteorol. 140 (1–4), 136–151, http://dx.doi.org/10.1016/j.agrformet.2006.08.008.
Kelliher, F.M., Leuning, R., Raupach, M.R., Schulze, E.-D., 1995. Maximum conductances for evaporation from global vegetation types. Agric. For. Meteorol. 73 (1), 1–16.
Lai, C.-T., Katul, G., Oren, R., Ellsworth, D., Schäfer, K., 2000. Modeling CO_2 and water vapor turbulent flux distributions within a forest canopy. J. Geophys. Res.: Atmos. 105 (D21), 26333–26351, http://dx.doi.org/10.1029/2000JD900468.
Liu, J., Chen, J.M., Cihlar, J., 2003. Mapping evapotranspiration based on remote sensing: an application to Canada's landmass. Water Resour. Res. 39 (7), 1189.
Liu, J., Chen, J.M., Cihlar, J., Chen, W., 1999. Net primary productivity distribution in the BOREAS region from a process model using satellite and surface data. J. Geophys. Res. 104 (D22), 27735–27754.
Liu, J., Chen, J.M., Cihlar, J., Park, W.M., 1997. A process-based boreal ecosystem productivity simulator using remote sensing inputs. Remote Sens. Environ. 62 (2), 158–175, http://dx.doi.org/10.1016/S0034-4257(97)00089-8.
Liu, Y., Zhou, Y., Ju, W., Chen, J., Wang, S., He, H., . . . Hao, Y., 2013. Evapotranspiration and water yield over China's landmass from 2000 to 2010. Hydrol. Earth Syst. Sci. 17 (12), 4957–4980, http://dx.doi.org/10.5194/hess-17-4957-2013.
Monteith, J.L., 1965. Evaporation and environment. In: Symp. Soc. Exp. Biol., vol. 19, p. 4.
Mu, Q., Zhao, M., Running, S.W., 2011. Improvements to a MODIS global terrestrial evapotranspiration algorithm. Remote Sens. Environ. 115 (8), 1781–1800.
Norman, J.M., 1982. Simulation of microclimates. In: Hatfield, J.L., Thomason, I.J. (Eds.), Biometeorology in Integrated Pest Management. Academic Press, New York, pp. 65–99.
Paw, U.K.T., Meyers, T.P., 1989. Investigations with a higher-order canopy turbulence model into mean source-sink levels and bulk canopy resistances. Agric. For. Meteorol. 47 (2), 259–271.
Potter, C.S., et al., 2001. Comparison of boreal ecosystem model sensitivity to variability in climate and forest site parameters. J. Geophys. Res. 106 (D24), 33671–33687.
Raupach, M.R., Finnigan, J.J., 1988. 'Single-layer models of evaporation from plant canopies are incorrect but useful, whereas multilayer models are correct but useless': discuss. Funct. Plant Biol. 15 (6), 705–716.
Running, S.W., Coughlan, J.C., 1988. A general model of forest ecosystem processes for regional applications I. Hydrologic balance, canopy gas exchange and primary production processes. Ecol. Model. 42 (2), 125–154.
Ryu, Y., Baldocchi, D.D., Kobayashi, H., van Ingen, C., Li, J., Black, T.A., . . . Roupsard, O., 2011. Integration of MODIS land and atmosphere products with a coupled-process model to estimate gross primary productivity and evapotranspiration from 1 km to global scales. Glob. Biogeochem. Cycl. 25 (4), 1–24, http://dx.doi.org/10.1029/2011GB004053.
Sellers, P.J., Dickinson, R.E., Randall, D.A., Betts, A.K., Hall, F.G., Berry, J.A., . . . Henderson-Sellers, A., 1997. Modeling the exchanges of energy, water, and carbon between continents and the atmosphere. Science 275 (5299), 502–509, http://dx.doi.org/10.1126/science.275.5299.502.
Sellers, P.J., Heiser, M.D., Hall, F.G., 1992. Relations between surface conductance and spectral vegetation indices at intermediate (100 m^2 to 15 km^2) length scales. J. Geophys. Res.: Atmos. 97 (D17), 19033–19059, http://dx.doi.org/10.1029/92JD01096.
Thomas, C.K., Law, B.E., Irvine, J., Martin, J.G., Pettijohn, J.C., Davis, K.J., 2009. Seasonal hydrology explains interannual and seasonal variation in carbon and water exchange in a semiarid mature ponderosa pine forest in central Oregon. J. Geophys. Res.: Biogeosci. 114 (G4), 1–22, http://dx.doi.org/10.1029/2009JG001010.
Wang, K., Dickinson, R.E., 2012. A review of global terrestrial evapotranspiration: Observation, modeling, climatology, and climatic variability. Rev. Geophys. 50 (2), RG2005, http://dx.doi.org/10.1029/2011rg000373.
Wang, Q., Tenhunen, J., Falge, E., Bernhofer, C., Granier, A., Vesala, T., 2004. Simulation and scaling of temporal variation in gross primary production for coniferous and deciduous temperate forests. Glob. Change Biol. 10 (1), 37–51, http://dx.doi.org/10.1111/j.1365-2486.2003.00716.x.
Yuan, W., Liu, S., Liu, H., Randerson, J.T., Yu, G., Tieszen, L.L., 2010. Impacts of precipitation seasonality and ecosystem types on evapotranspiration in the Yukon River Basin, Alaska. Water Resour. Res. 46 (2), W02514, http://dx.doi.org/10.1029/2009wr008119.
Zhou, Y., Zhu, Q., Chen, J.M., Wang, Y.Q., Liu, J., Sun, R., Tang, S., 2007. Observation and simulation of net primary productivity in Qilian Mountain, western China. J. Environ. Manag. 85 (3), 574–584, http://dx.doi.org/10.1016/j.jenvman.2006.04.024.